Supporting Information

COPPER-NITROXIDE BASED BREATHING CRYSTALS: UNIFIED MECHANISM OF GRADUAL MAGNETOSTRUCTURAL TRANSITION SUPPORTED BY QUANTUM CHEMISTRY CALCULATIONS

Rocío Sánchez-de-Armas,[1] Norge Cruz Hernández,[2] and Carmen J. Calzado[1]*

[1]Departamento de Química Física. Universidad de Sevilla. 41012. Spain.

[2]Departamento de Física Aplicada I, Escuela Politécnica Superior, Universidad de Sevilla, 41011, Spain

*corresponding author: calzado@us.es

Table S1. Cu-O bond distances (Å) within the spin triads for compound **1** from X-Ray data,[1,2] weight fractions of the low temperature phase (w) and Cu−O Distances (d_T) for structures in the transition region estimated as an weighted average of the corresponding distances in the LT and HT Structures (eq. 7 in main text). Relative (%) and Absolute errors (Å).

Table S2. Cu-O bond distances (Å) within the spin triads for compound **2** from X-Ray data,[1,2] weight fractions of the low temperature phase (w) and Cu−O Distances (d_T) for structures in the transition region estimated as an weighted average of the corresponding distances in the LT and HT Structures (eq. 7 in main text). Relative (%) and Absolute errors (Å).

Table S3. Cu-O bond distances (Å) within the spin triads for compound **3** from X-Ray data,[1,2] weight fractions of the low temperature phase (w) and Cu−O Distances (d_T) for structures in the transition region estimated as an weighted average of the corresponding distances in the LT and HT Structures (eq. 7 in main text). Relative (%) and Absolute errors (Å).

Figure S1. (a) View along the *a* axis of the unit cell for compound **1**, in the middle the NIT-Cu-NIT spin triad, and in the corners the one-spin CuO_4N_2 clusters. (b) Schematic representation of the three considered magnetic solutions for compound 1. Blue and red arrows represent, respectively, the Cu and NIT spins of the three-spin cluster (spin triad). Black arrow represents the one-spin CuO_4N_2 cluster. Dotted red lines represent the limits of the unit cell. (c) Spin density maps for the AFM, AFM2 and FM solutions of compound **1** at 125K. Blue and yellow contours have been used to distinguish between positive and negative spin density. View along the *a* axis.

Figure S2. (left) Model employed for the evaluation of the interchain interaction and (right) symmetry-adapted combination of the magnetic orbitals centered on the nitronyl nitroxide moieties (right) for (a) compound **2** at 295K and (b) compound **3** at 293K.

Figure S3. Spin density maps for the AFM solution of $Cu(hfac)_2L^{Bu}\cdot 0.5\ C_8H_{18}$ (**1**) complex at different temperatures.

Table S1. Cu-O bond distances (Å) within the spin triads for compound **1** from X-Ray data,[1,2] weight fractions of the low temperature phase (w) and Cu−O distances (d_T) for structures in the transition region estimated as a weighted average of the corresponding distances in the LT and HT structures (eq. 7 in main text). Relative (%) and absolute errors (Å).

X-Ray data							
T/K	**100 (LT)**	**125**	**145**	**155**	**175**	**240**	**295 (HT)**
$Cu\text{-}O_{NO}$	2,034	2,122	2,189	2,26	2,307	2,334	2,352
$Cu\text{-}O_{hfac1}$	1,998	1,993	1,981	1,969	1,965	1,964	1,960
$Cu\text{-}O_{hfac2}$	2,201	2,108	2,06	2,011	1,99	1,953	1,971
w	1	0,6812	0,4702	0,2495	0,1214	0,0104	0
Weighted LT and HT structures							
T/K	**100**	**125**	**145**	**155**	**175**	**240**	**295**
$Cu\text{-}O_{NO}$	2,034	2,135	2,202	2,273	2,313	2,349	2,352
$Cu\text{-}O_{hfac1}$	1,998	1,986	1,978	1,969	1,965	1,960	1,960
$Cu\text{-}O_{hfac2}$	2,201	2,128	2,079	2,028	1,999	1,973	1,971
relative error (%)							
$Cu\text{-}O_{NO}$		0,630	0,616	0,560	0,277	0,630	
$Cu\text{-}O_{hfac1}$		0,357	0,158	0,024	0,020	0,183	
$Cu\text{-}O_{hfac2}$		0,934	0,929	0,864	0,448	1,044	
absolute error (Å)							
$Cu\text{-}O_{NO}$		0,013	0,013	0,013	0,006	0,015	
$Cu\text{-}O_{hfac1}$		-0,007	-0,003	0,001	0,000	0,004	
$Cu\text{-}O_{hfac2}$		0,020	0,019	0,017	0,009	0,020	

Table S2. Cu-O bond distances (Å) within the spin triads for compound **2** from X-Ray data,[1,2] weight fractions of the low temperature phase (w) and Cu−O distances (d_T) for structures in the transition region estimated as a weighted average of the corresponding distances in the LT and HT structures (eq. 7 in main text). Relative (%) and absolute errors (Å).

X-Ray Data						
T/K	**60 (LT)**	**100**	**150**	**180**	**240**	**295(HT)**
Cu-O_{NO}	2,003	2,006	2,064	2,137	2,206	2,285
Cu-O_{hfac1}	1,963	1,951	1,959	1,973	1,975	1,964
Cu-O_{hfac2}	2,301	2,271	2,178	2,111	2,005	1,986
w	1	0,9425	0,6870	0,4537	0,1580	0
Weighted LT and HT structures						
Cu-O_{NO}		2,019	2,091	2,157	2,240	
Cu-O_{hfac1}		1,963	1,963	1,964	1,964	
Cu-O_{hfac2}		2,283	2,202	2,129	2,036	
relative error (%)						
Cu-O_{NO}		0,659	1,321	0,938	1,561	
Cu-O_{hfac1}		0,618	0,220	0,479	0,565	
Cu-O_{hfac2}		0,523	1,121	0,849	1,535	
absolute error (Å)						
Cu-O_{NO}		0,013	0,027	0,020	0,034	
Cu-O_{hfac1}		0,012	0,004	0,009	0,011	
Cu-O_{hfac2}		0,012	0,024	0,018	0,031	

Table S3. Cu-O bond distances (Å) within the spin triads for compound **3** from X-Ray data,[1,2] weight fractions of the low temperature phase (w) and Cu−O distances (d_T) for structures in the transition region estimated as a weighted average of the corresponding distances in the LT and HT structures (eq. 7 in main text). Relative (%) and absolute errors (Å).

X-Ray Data													
T/K	**50(LT)**	**115**	**145**	**175**	**195**	**205**	**215**	**220**	**225**	**229**	**232**	**240**	**293(HT)**
Cu-O_{NO}	1,994	2,022	2,045	2,086	2,114	2,140	2,156	2,17	2,195	2,217	2,231	2,256	2,318
Cu-O_{hfac1}	1,949	1,964	1,961	1,962	1,958	1,961	1,958	1,960	1,964	1,957	1,958	1,96	1,955
Cu-O_{hfac2}	2,274	2,278	2,239	2,1925	2,14	2,13	2,109	2,097	2,079	2,049	2,046	2,018	1,975
w	1	0,9589	0,8600	0,7201	0,5928	0,5349	0,4760	0,4341	0,3647	0,2821	0,2541	0,1693	0
Weighted LT and HT structures													
Cu-O_{NO}		2,007	2,039	2,085	2,126	2,145	2,164	2,177	2,200	2,227	2,236	2,263	
Cu-O_{hfac1}		1,949	1,950	1,951	1,951	1,952	1,952	1,952	1,953	1,953	1,953	1,954	
Cu-O_{hfac2}		2,262	2,232	2,190	2,152	2,135	2,117	2,105	2,084	2,059	2,051	2,026	
relative error (%)													
Cu-O_{NO}		0,751	0,300	0,087	0,541	0,220	0,361	0,338	0,221	0,433	0,209	0,317	
Cu-O_{hfac1}		0,776	0,569	0,552	0,360	0,444	0,299	0,388	0,570	0,189	0,231	0,307	
Cu-O_{hfac2}		0,736	0,307	0,100	0,572	0,231	0,394	0,372	0,242	0,505	0,243	0,378	
absolute error (Å)													
Cu-O_{NO}		0,015	0,006	0,002	0,011	0,005	0,008	0,007	0,005	0,010	0,005	0,007	
Cu-O_{hfac1}		0,015	0,011	0,011	0,007	0,009	0,006	0,008	0,011	0,004	0,005	0,006	
Cu-O_{hfac2}		0,017	0,007	0,002	0,012	0,005	0,008	0,008	0,005	0,010	0,005	0,008	

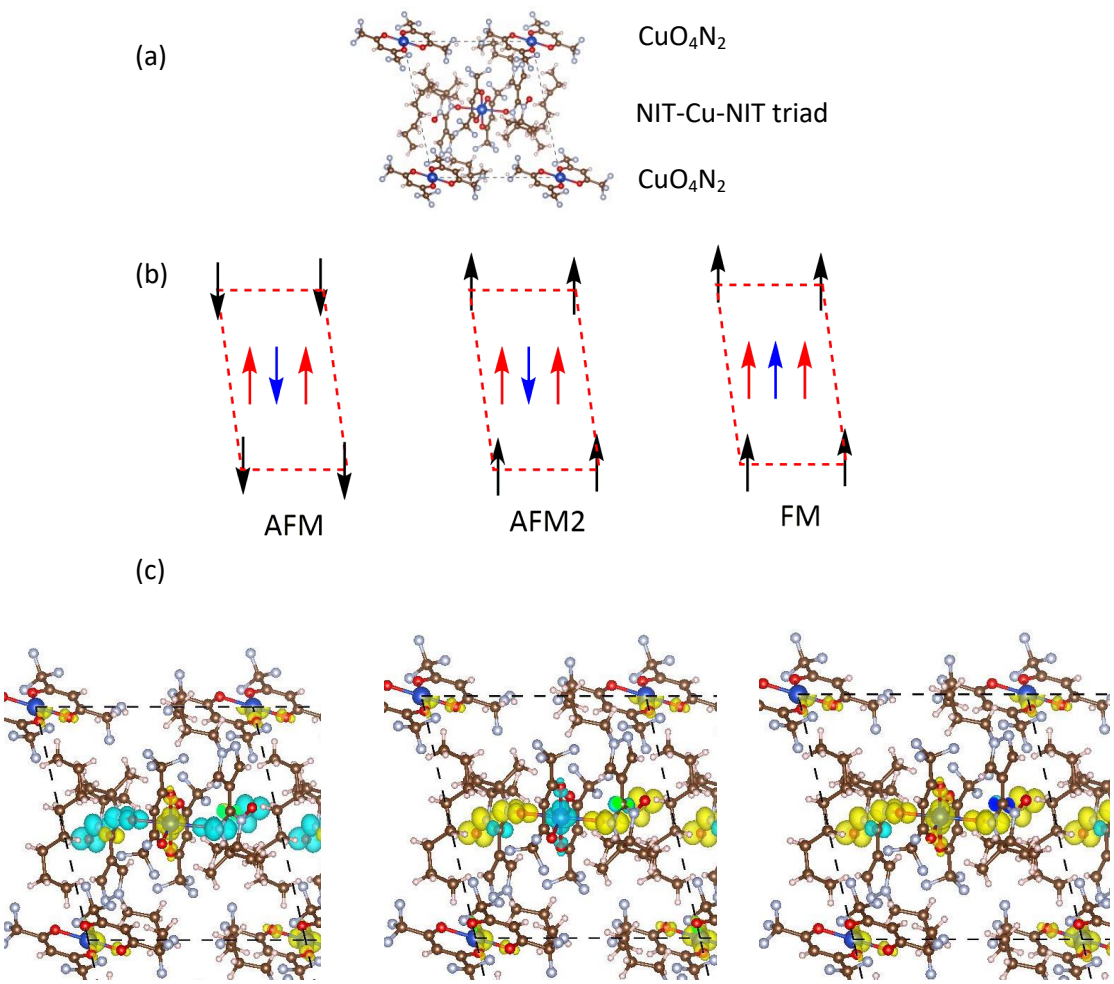

Figure S1. (a) View along the *a* axis of the unit cell for compound **1**, in the middle the NIT-Cu-NIT spin triad, and in the corners the one-spin CuO_4N_2 clusters. (b) Schematic representation of the three considered magnetic solutions for compound 1. Blue and red arrows represent, respectively, the Cu and NIT spins of the three-spin cluster (spin triad). Black arrow represents the one-spin CuO_4N_2 cluster. Dotted red lines represent the limits of the unit cell. (c) Spin density maps for the AFM, AFM2 and FM solutions of compound **1** at 125K. Blue and yellow contours have been used to distinguish between positive and negative spin density. View along the *a* axis.

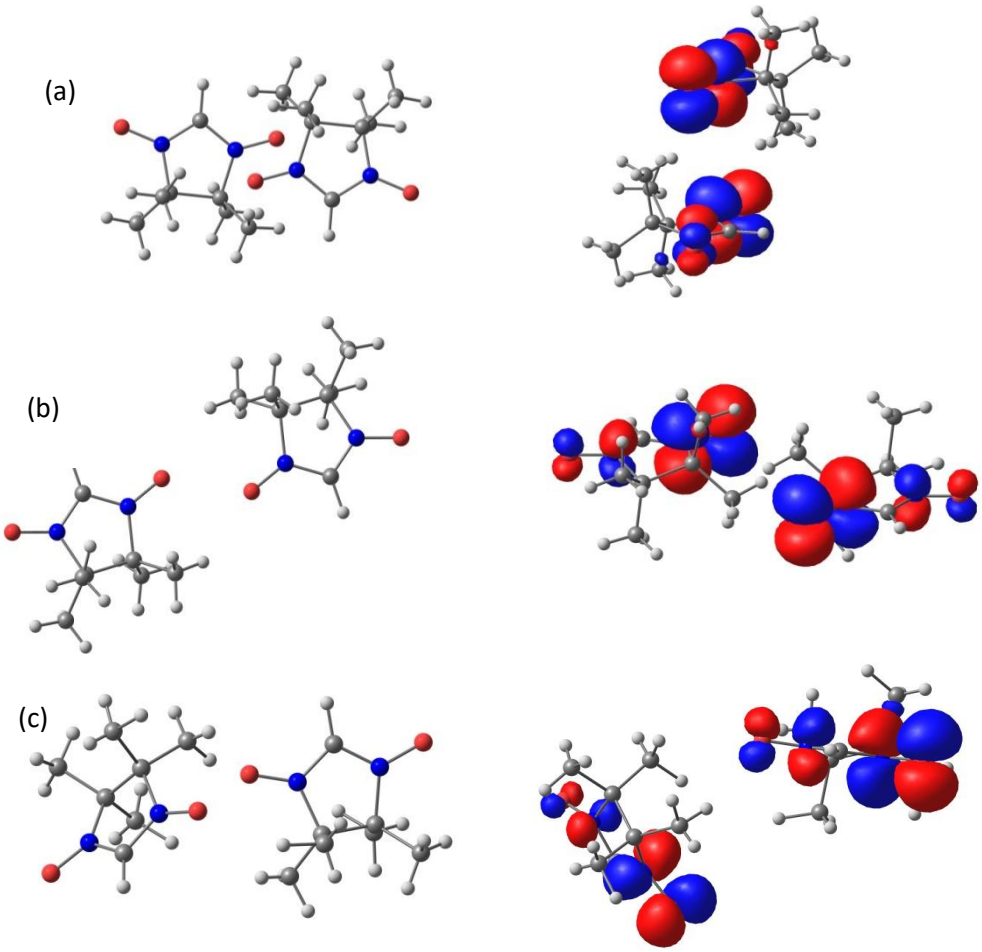

Figure S2. (left) Model employed for the evaluation of the interchain interaction and (right) symmetry-adapted combination of the magnetic orbitals centered on the nitronyl nitroxide moieties (right) for (a) compound **1** at 295K, (b) compound **2** at 295K and (b) compound **3** at 293K . Red, blue, grey and white balls represent O, N, C and H atoms, respectively.

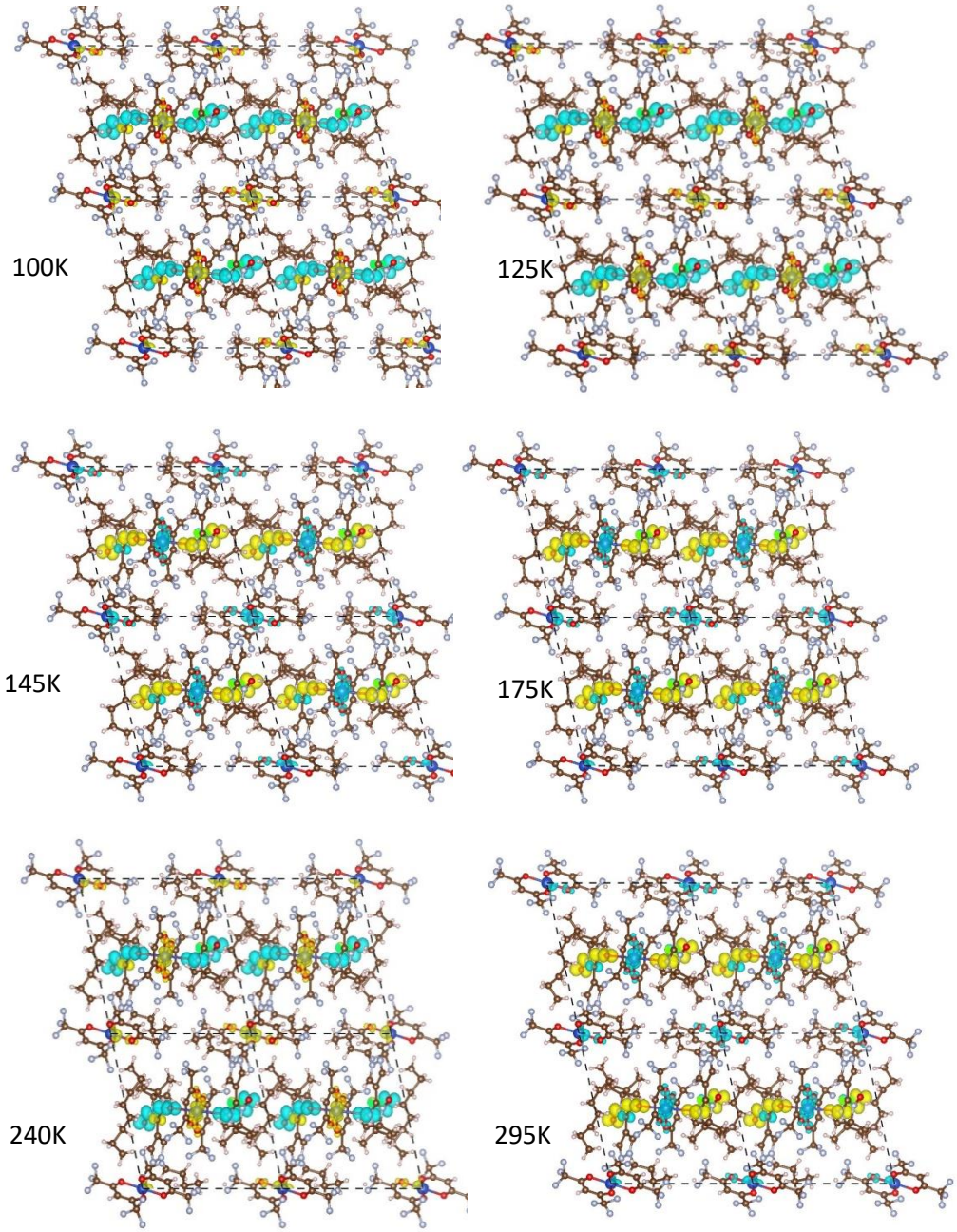

Figure S3. Spin density maps for the AFM solution of $Cu(hfac)_2L^{Bu}\cdot 0.5\ C_8H_{18}$ (**1**) complex at different temperatures. Four unit cells are represented, delimited by a dashed line. View along the *a* axis. Yellow and blue surfaces correspond to positive and negative spin density, respectively.

1. Fedin, M.; Veber, S.; Gromov, I.; Maryunina, K.; Fokin, S.; Romanenko, G.; Sagdeev, R.; Ovcharenko, V.; Bagryanskaya, E., Thermally Induced Spin Transitions in Nitroxide−Copper(II)−Nitroxide Spin Triads Studied by EPR. *Inorganic Chemistry* 2007, *46* (26), 11405-11415.
2. Fedin, M. V.; Veber, S. L.; Romanenko, G. V.; Ovcharenko, V. I.; Sagdeev, R. Z.; Klihm, G.; Reijerse, E.; Lubitz, W.; Bagryanskaya, E. G., Dynamic mixing processes in spin triads of "breathing crystals'' Cu(hfac)(2)L-R: a multifrequency EPR study at 34, 122 and 244 GHz. *Physical Chemistry Chemical Physics* 2009, *11* (31), 6654-6663.